Volume 4 / Issue 7/ July 2026
ISSN:2584-2706
International Journal of Modern Science and Research Technology
DOI: https://doi.org/10.67317/IJMSRT26JUL092

Land use and Land Cover Change Detection and Impacts on Biodiversity due to Rohingya Settlement: A GIS and ENVI- Based Imagery Analysis in the South-Eastern Region of Bangladesh

Nurul Hamid; Md. Redwanur Rahman*
Institute of Environmental Science, University of Rajshahi,
Rajshahi-6205, Bangladesh

*Corresponding Author

Abstract

The rapid expansion of settlements in the Southeastern region of Bangladesh has led to significant changes in Land Use and Land Cover (LULC), posing critical threats to biodiversity and ecosystem stability. This study quantifies and analyzes the spatial and temporal dynamics of Land Use and Land Cover (LULC) changes and their impacts on biodiversity in Cox's Bazar, Bangladesh, from 2015 to 2025 using advanced geospatial techniques. It further predicts future LULC trends and evaluates their potential consequences for biodiversity conservation in the region.The area has witnessed unprecedented settlement expansion, especially after the influx of Rohingya refugees in 2017, leading to significant ecological disruptions.

Utilizing multi-temporal satellite imagery from Landsat-8 & Landsat-9, four major LULC classification has been performed through supervised Classification.The classes have been identified and analyzed using ENVI for spatial pattern recognition. Change detection and prediction analysis for next 5 years have been conducted. The results of this study reveals a non-linear pattern of forest loss, predicting a 45.93% reduction in high-density vegetation by 2030, contrasted with a 9.84% increase in built-up areas. The findings are supported by a highly dependable LULC classification, attaining an overall accuracy of 88.75% and a Kappa coefficient of 0.841, thereby substantiating the evaluation of biodiversity risks. In this study, biodiversity indicators were evaluated through Bayesian Time Series Analysis integrated with a Cellular Automata (CA)-Markov Model. The application of GIS and remote sensing tools demonstrates their efficacy in tracking environmental changes and supports data-driven conservation planning in rapidly urbanizing regions.

Keywords:
LULC,ENVI Classification, GIS Imagery, Biodiversity Impacts, Degradation

1.0 Introduction

Massive shifts in land use and land cover (LULC) have occurred in areas like Teknaf, Ukhiya and Teknaf Wildlife Sanctuary after the largescale arrival of Rohingya refugees in southeast Bangladesh in2017.

The swift and extensive creation of refugee settlements serves as a significant accelerator for changes in land use and land cover (LULC), frequently resulting in serious repercussions for ecologically vulnerable regions (Bashir et al., 2023). These regions are biodiversity hotspots, harboring delicate flora and animals, and function as essential wildlife corridors. Numerous recent studies employing GIS and remote sensing have quantified these alterations in the terrain. For instance, the study on Environmental Change Detection via Remote Sensing Techniques (Hossain & Moniruzzaman, 2021) utilized Landsat 5 TM and Landsat 8 OLI/TIRS imagery to demonstrate that from 1990 to 2020, vegetation in Ukhia and Teknaf diminished by approximately 5,181 hectares (around 17%), whereas settlement and refugee camp areas experienced a significant increase, with the refugee camp category rising by approximately 582%. Measuring these alterations is crucial for comprehending historical effects and predicting future landscape developments to guide proactive conservation and land-use strategies. A further study, Spatio-temporal Variation of Land Use and Land Cover Changes…, examined the Kutupalong Mega Camp pre- and post-2017; it recorded an inverse correlation between forest cover and settlement expansion, indicating a decrease in forest cover due to influx-driven urban development. A geo-spatial investigation of the Teknaf Wildlife Sanctuary (Miah, Hossain & Ali, 2024) identified a loss of around 1,389 hectares (≈ 12% of dense forest) from 1991 to 2021, utilizing supervised classification through satellite imagery and GIS techniques. Although these studies establish an essential historical baseline, there is an urgent necessity to progress beyond descriptive change detection to predictive modeling that can forecast future land use and land cover scenarios based on present patterns. Time series analysis provides a comprehensive framework for forecasting, facilitating the detection of underlying patterns and the prediction of future changes (Hasan et al., 2020). Bayesian Structural Time Series (BSTS) models are notably effective in this setting, offering a probabilistic forecasting method capable of managing intricate time series data and producing forecasts with quantifiable uncertainty (Brodersen et al., 2015). This is essential for formulating resilient, evidence-driven land management strategies.

1.1 Objectives

The main objectives of the research are:

i) To quantify the extent of land use and land cover (LULC) changes: This study quantifies the extent of land use and land cover (LULC) changes including forest, shrubland, agricultural land and built-up areas-in Teknaf, Ukhiya, and surrounding southeastern Bangladesh through a comparative analysis of pre- and post-settlement satellite imagery.

ii) To assess the trends and prediction of land use land cover change utilizing BSTS Model: This study analyzes historical land use and land cover (LULC) change to identify trends and applies a Bayesian Structural Time Series (BSTS) model to generate robust, probabilistic forecasts for informing sustainable land management.

iii.) To verify the cross validation of the trends and prediction accuracy: This study rigorously cross-validates trends and prediction accuracy to assess the model's robustness and out-of-sample forecasting performance.

This research offers a thorough analysis of land use and land cover (LULC) dynamics by combining a strong GIS and ENVI-based assessment of multi-temporal satellite images with sophisticated statistical predictions. This study initially categorizes land to delineate historical habitat loss and degradation, assessing its subsequent impacts on biodiversity. Subsequent to this diagnostic investigation, a Bayesian Structural Time Series (BSTS) model is utilized to forecast future land use and land cover (LULC) alterations.The resulting probabilistic estimates aim to produce strong, evidence-based insights that will guide the development of sustainable resource management strategies, effective conservation priorities, and focused rehabilitation initiatives for this extremely vulnerable region.

2.0 Materials and methods

2.1 Study Area

This study was conducted in the southeastern coastal region of Bangladesh, which is in the sub-districts of Ukhiya and Teknaf beneath Cox's Bazar district. The research area is geographically situated between about 20°44′N and 21°20′N latitude, and 92°05′E and 92°20′E longitude, encompassing a region defined by steep terrain, tropical forest ecosystems, and a narrow coastal plain. Ukhiya and Teknaf hold global significance due to the construction of the world's largest refugee camp, which has accommodated over one million Rohingya individuals since 2017. The swift and extensive settlement has imposed significant strain on local land use and land cover (LULC), resulting in deforestation, conversion of agricultural land, and loss of biodiversity. The area was formerly characterized by forest reserves, hill ecosystems, and agricultural fields; however, recent human activities, especially in the Kutupalong and Nayapara camps, have significantly transformed the natural environment. The spatial transition renders Ukhiya and Teknaf essential for geo-spatial analysis to identify land use and land cover changes and evaluate their ecological and socio-environmental consequences within Cox's Bazar district.

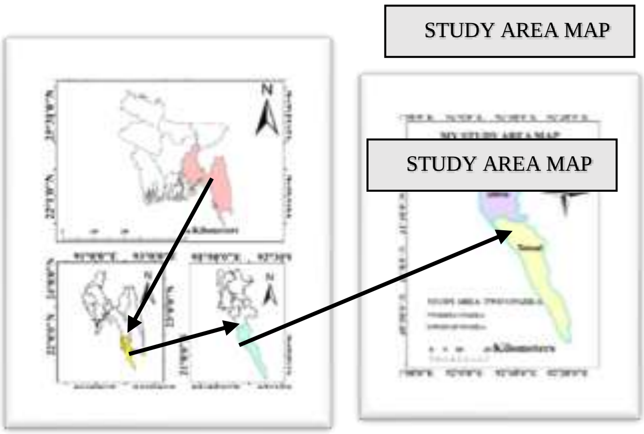

Figure-1: The map (a) showing the division of Bangladesh and (b) showing the location of Ukhiya and Teknaf sub-district

2.2 Data source, gathering and analysis

The principal LULC data source for the study was USGS Landsat OLI/TIRS 8 and 9 imagery, which included the south-eastern region of Bangladesh. Prior to classification, atmospheric correction and Band 1–7 stacking were implemented in ArcGIS for image pre-processing.The assessment of the risk of settlements to natural hazards and to provide data regarding forest depletion and changes of physiography. It is difficult to access cloud-free images of the area because of climatic monsoon trend which exist between March to November (Hassan et al.,2018). However, we have used maximum cloudfree images for all the years (Quader et al.,2020). In ENVI, a supervised maximum likelihood classification (MLC) was conducted to identify four land cover classes: aquatic bodies, built-up areas, low vegetation, and high vegetation. The classification accuracy was verified using kappa statistics, and post-processing mapping was implemented to enhance the accuracy. Bayesian time series modeling, statistical graphing, and TerrSet change detection with prediction analysis were implemented to evaluate temporal dynamics. The incorporated procedures were summarized in a workflow presentation, while cross-validation techniques improved model reliability. This combined approach enabled the precise identification of LULC alterations and their effects on biodiversity as a result of the expansion of Rohingya settlements.

2.3 Data Collection and Pre-processing for Geo-Spatial Analysis

This research utilized multispectral datasets from the Landsat-8 Operational Land Imager (OLI) and Landsat-9, acquired from the United States Geological Survey (USGS) Earth Explorer portal, which offers free and reliable satellite archives commonly employed in land use and land cover (LULC) analysis (USGS, 2023). To guarantee radiometric accuracy, atmospheric correction was executed in ArcGIS employing established procedures to reduce air scattering and absorption effects, hence improving surface reflectance values (Song et al., 2001). The research area encompasses two adjacent path/row scenes (136/045 and 135/046), necessitating mosaicking to produce a continuous raster composite that encompasses the entire region (Chander et al., 2009). The mosaicked picture was subsequently geocliped to the specified study border to reduce superfluous data and enhance computational efficiency. From this dataset, primary preprocessed bands pertinent for differentiating vegetation, aquatic environments, and constructed characteristics were extracted. The preprocessed images were ultimately produced in Tagged Image File Format (TIFF) to ensure interoperability with ENVI software for supervised classification (Jensen, 2015). These approaches yielded spatially precise and spectrally uniform datasets, establishing a solid basis for later geo-spatial and biodiversity impact evaluations.

2.4 Workflow of Satellite Imagery Data: Preprocessing, Processing and Postprocessing

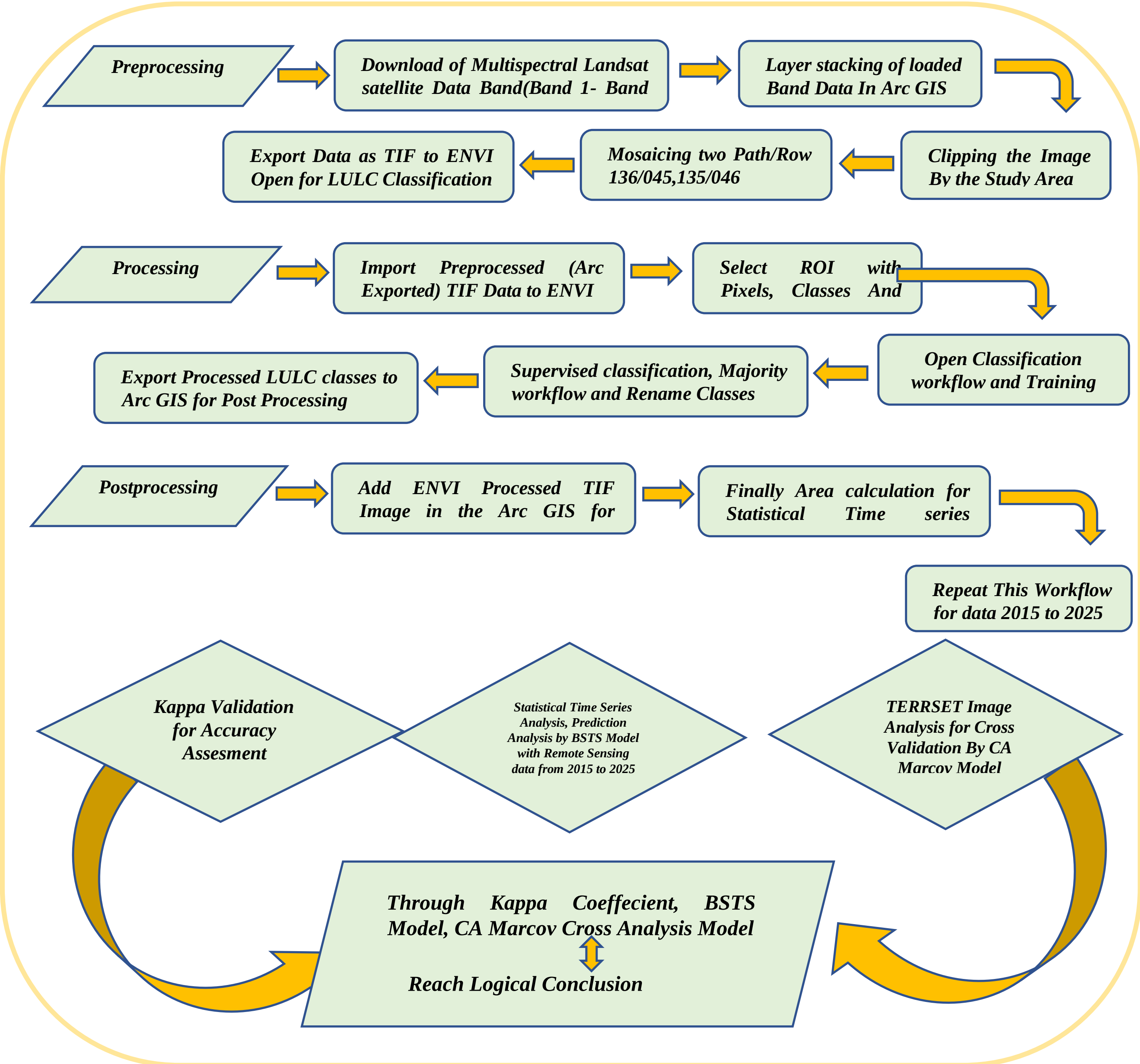

Figure-2: **Overall research Workflow of Satellite Imagery Data: Preprocessing, Processing and Postprocessing**

Table-1: Data sources of satellite images.Satellite images has been downloaded free from USGS global visualization viewer and humanitarian data exchange websites:

Data types	Acquisition Date	Resolution	Row/path	Cloud cover	Data Source
Landsat 8 OLI/TIRS	**21/11/2015**	**30 m x 30 m**	**136/045**	**0.27**	United States Geological Survey (USGS) Global Visualization Viewer https://earthexplorer.usgs.gov/login
Landsat 8 OLI/TIRS	**30/11/2015**	**30 m x 30 m**	**135/046**	**0.11**	United States Geological Survey (USGS) Global Visualization Viewer https://earthexplorer.usgs.gov/login
Landsat 8 OLI/TIRS	**23/11/2016**	**30 m x 30 m**	**136/045**	**0.95**	United States Geological Survey (USGS) Global Visualization Viewer https://earthexplorer.usgs.gov/login
Landsat 8 OLI/TIRS	**16/11/2016**	**30 m x 30 m**	**135/046**	**2.18**	United States Geological Survey (USGS) Global Visualization Viewer https://earthexplorer.usgs.gov/login
Landsat 8 OLI/TIRS	**26/11/2017**	**30 m x 30 m**	**136/045**	**2.37**	United States Geological Survey (USGS) Global Visualization Viewer https://earthexplorer.usgs.gov/login
Landsat 8 OLI/TIRS	**19/11/2017**	**30 m x 30 m**	**135/046**	**1.91**	United States Geological Survey (USGS) Global Visualization Viewer https://earthexplorer.usgs.gov/login
Landsat 8 OLI/TIRS	**29/11/2018**	**30 m x 30 m**	**136/045**	**0.00**	United States Geological Survey (USGS) Global Visualization Viewer https://earthexplorer.usgs.gov/login
Landsat 8 OLI/TIRS	**22/11/2018**	**30 m x 30 m**	**135/046**	**0.12**	United States Geological Survey (USGS) Global Visualization Viewer https://earthexplorer.usgs.gov/login
Landsat 8	**16/11/2019**	**30 m x 30 m**	**136/045**	**0.01**	United States Geological Survey (USGS)

OLI/TIRS					Global Visualization Viewer https://earthexplorer.usgs.gov/login
Landsat 8 OLI/TIRS	**25/11/2019**	**30 m x 30 m**	**135/046**	**0.37**	United States Geological Survey (USGS) Global Visualization Viewer https://earthexplorer.usgs.gov/login
Landsat 8 OLI/TIRS	**18/11/2020**	**30 m x 30 m**	**136/045**	**0.41**	United States Geological Survey (USGS) Global Visualization Viewer https://earthexplorer.usgs.gov/login
Landsat 8 OLI/TIRS	**27/11/2020**	**30 m x 30 m**	**135/046**	**0.34**	United States Geological Survey (USGS) Global Visualization Viewer https://earthexplorer.usgs.gov/login
Landsat 9 OLI/TIRS	**19/11/2021**	**30 m x 30 m**	**136/045**	**0.16**	United States Geological Survey (USGS) Global Visualization Viewer https://earthexplorer.usgs.gov/login
Landsat 8 OLI/TIRS	**30/11/2021**	**30 m x 30 m**	**135/046**	**0.56**	United States Geological Survey (USGS) Global Visualization Viewer https://earthexplorer.usgs.gov/login
Landsat 8 OLI/TIRS	**24/11/2022**	**30 m x 30 m**	**136/045**	**1.27**	United States Geological Survey (USGS) Global Visualization Viewer https://earthexplorer.usgs.gov/login
Landsat 9 OLI/TIRS	**09/11/2022**	**30 m x 30 m**	**135/046**	**1.61**	United States Geological Survey (USGS) Global Visualization Viewer https://earthexplorer.usgs.gov/login
Landsat 9 OLI/TIRS	**03/11/2023**	**30 m x 30 m**	**136/045**	**0.41**	United States Geological Survey (USGS) Global Visualization Viewer https://earthexplorer.usgs.gov/login
Landsat 9 OLI/TIRS	**28/11/2023**	**30 m x 30 m**	**135/046**	**0.01**	United States Geological Survey (USGS) Global Visualization Viewer https://earthexplorer.usgs.gov/login

ISSN:2584-2706 DOI: https://doi.org/10.67317/IJMSRT26JUL092

Landsat 8 OLI/TIRS	**13/11/2024**	**30 m x 30 m**	**136/045**	**2.26**	United States Geological Survey (USGS) Global Visualization Viewer https://earthexplorer.usgs.gov/login
Landsat 8 OLI/TIRS	**22/11/2024**	**30 m x 30 m**	**135/046**	**1.93**	United States Geological Survey (USGS) Global Visualization Viewer https://earthexplorer.usgs.gov/login
Landsat 8 OLI/TIRS	**05/03/2025**	**30 m x 30 m**	**136/045**	**1.47**	United States Geological Survey (USGS) Global Visualization Viewer https://earthexplorer.usgs.gov/login
Landsat 9 OLI/TIRS	**06/03/2025**	**30 m x 30 m**	**136/045**	**0.27**	United States Geological Survey (USGS) Global Visualization Viewer https://earthexplorer.usgs.gov/login

3.1 Post Processed Sattelite Imagery Data

3.1 Post Processed Sattelite Imagery Data Analysis

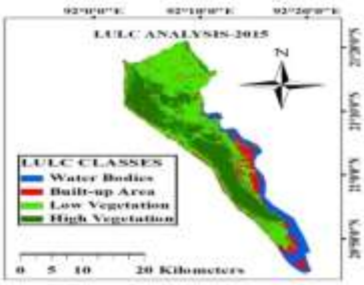

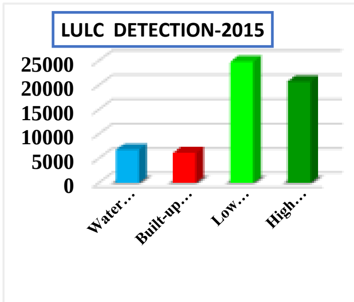

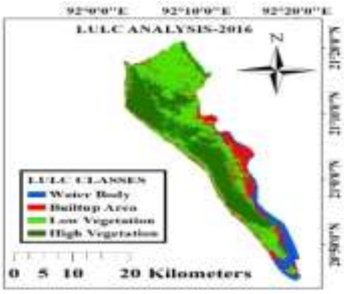

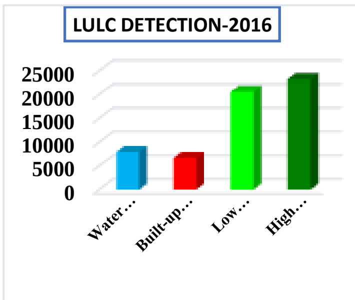

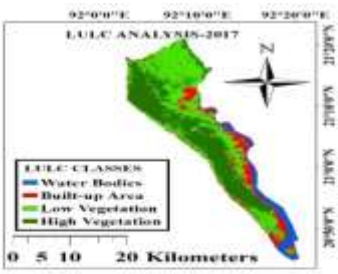

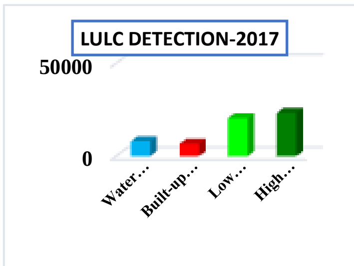

ISSN:2584-2706 DOI: https://doi.org/10.67317/IJMSRT26JUL092

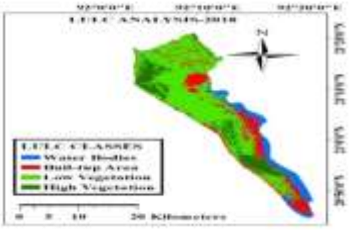

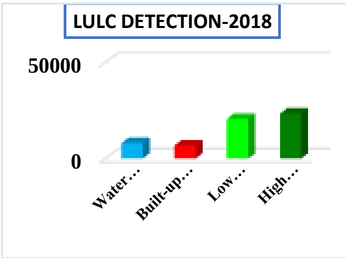

Figure-3: "The above figure simultaneously represents the LULC imagery change analysis and the bar diagrammatic change detection ratio from 2015 to 2018"

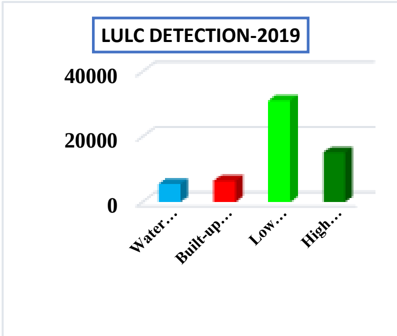

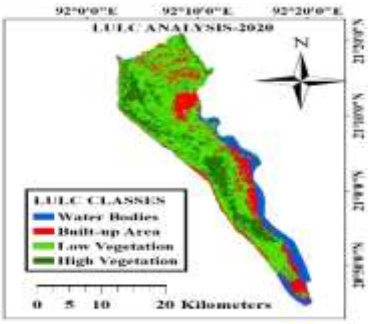

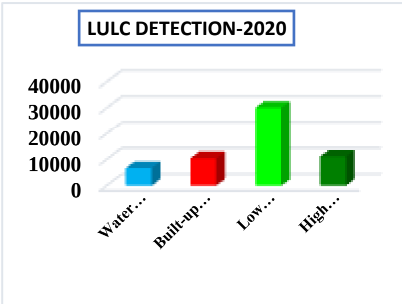

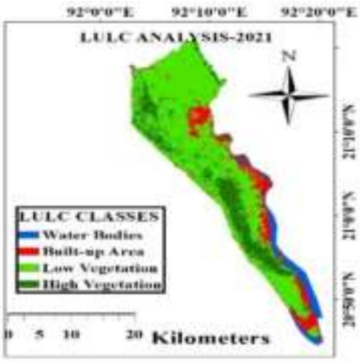

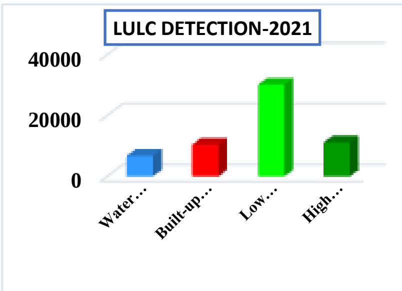

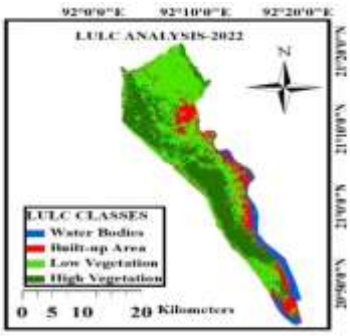

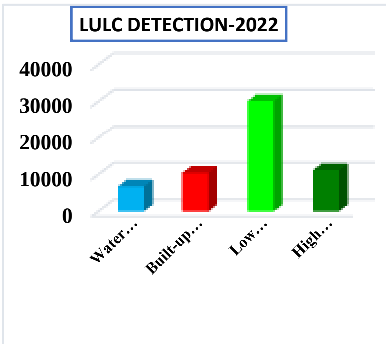

ISSN:2584-2706 DOI: https://doi.org/10.67317/IJMSRT26JUL092

Figure-4: "The above figure simultaneously represents the LULC imagery change analysis and the bar diagrammatic change detection ratio from 2019 to 2022"

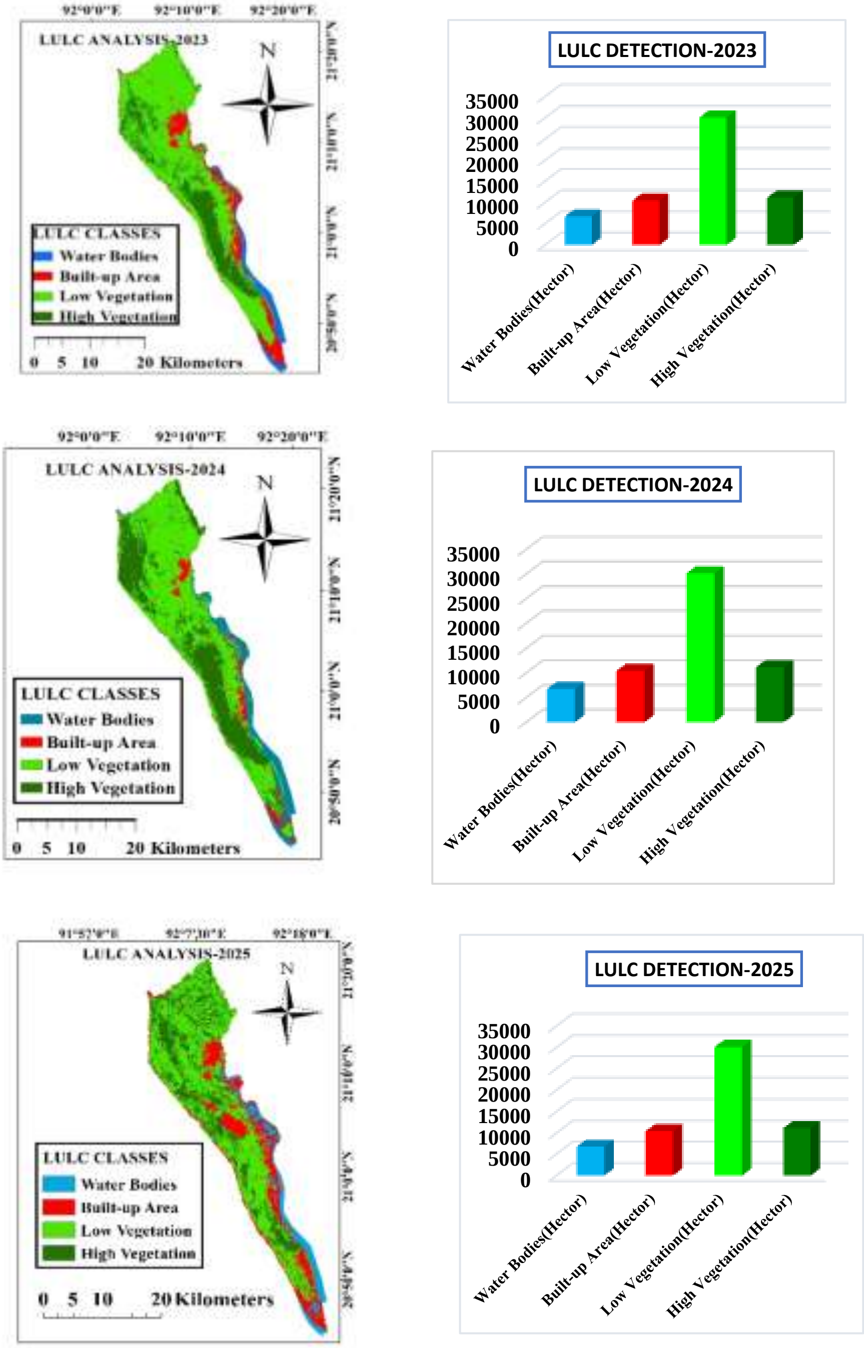

Figure-5 : "The above figure simultaneously represents the LULC imagery change analysis and the bar diagrammatic change detection ratio from 2023 to 2025"

The spatial extent of the Rohingya settlement in the Ukhiya and Teknaf sub-districts was analyzed using multi-temporal satellite imagery from 2015 to 2025, as depicted in Figures 3–5. The datasets underwent post-processing in ENVI software, utilizing the Maximum Likelihood Classification (MLC) approach to ascertain Land Use and Land Cover (LULC) classes. To evaluate the ecological consequences of land use and land cover dynamics on forest vegetation and related biodiversity, four primary categories were identified: water bodies, built-up area, low vegetation, and high vegetation.

The temporal analysis reveals that urban areas markedly grew from 2017 to 2018, coinciding with the peak of settlement influx during the 2017 Rohingya crisis (Figure 3). In contrast, forest vegetation demonstrated a persistent decline, with a significant decrease anticipated by 2025. Notwithstanding a slight resurgence in low vegetation in recent years, the degree of regrowth is inadequate relative to the scale of human encroachment. Water bodies exhibited a temporary decline during the initial period of settlement expansion, thereafter stabilizing during the following five to six years, as illustrated in Figures 4 and 5. Similar land use and land cover research validate these conclusions. Ahmed et al. (2022) reported a 48% reduction in forest cover and a 32% expansion of built-up area in the Teknaf Peninsula from 2010 to 2020, consistent with the trajectory seen in this study. Rahman et al. (2021) also identified a 39.2% reduction in dense woodland attributable to the proliferation of temporary camps and road infrastructure. Hassan et al. (2020) revealed increased deforestation and fragmentation, particularly in protected forest reserves, utilizing TerrSet and ArcGIS-based change detection. Furthermore, Islam et al. (2023) demonstrated that NDVI values in Ukhiya significantly decreased from 0.62 to 0.38 between 2016 and 2018, corroborating vegetative stress resulting from settlement-induced land alteration.

The comparative observations reveal a persistent trend of fast land use and land cover change, propelled by the growth of humanitarian settlements, which poses significant threats to forest integrity, watershed stability, and wildlife corridors (Rahman & Ahmed, 2021; UNDP, 2020). Despite the observable slight signals of vegetation regeneration in recent years, the overall spatial equilibrium remains disrupted, highlighting the necessity for sustained reforestation and spatial monitoring systems that use remote sensing and GIS-based ecological indicators.

Propelled by the growth of humanitarian settlements, which pose significant threats to forest integrity, watershed stability, and wildlife corridors (Rahman & Ahmed, 2021; UNDP, 2020). Despite the observable slight signals of vegetation regeneration in recent years, the overall spatial equilibrium remains disrupted, highlighting the necessity for sustained reforestation and spatial monitoring systems that use remote sensing and GIS-based ecological indicators.

Table-2: Extracted area data in hector from the catagorised four classes of LULC (2015 to 2025)

Year	Water Bodies(Hec)	Built-up Area(Hec)	Low Vegetation (Hec)	High Vegetation (Hec)	Total (Hector)
2015	6766	6134	24820	20770	58490
2016	4827	7622	23224	22817	58490
2017	5023	7299	22772	23396	58490
2018	6903	10406	31828	9353	58490
2019	5583	6519	31146	15242	58490
2020	6758	10444	30139	11149	58490
2021	4056	7259	36115	11060	58490
2022	4545	7712	25911	20322	58490
2023	3955	7570	35456	11509	58490
2024	6585	3312	30918	17675	58490

2025	**7925**	**6705**	**20557**	**23303**	**58490**

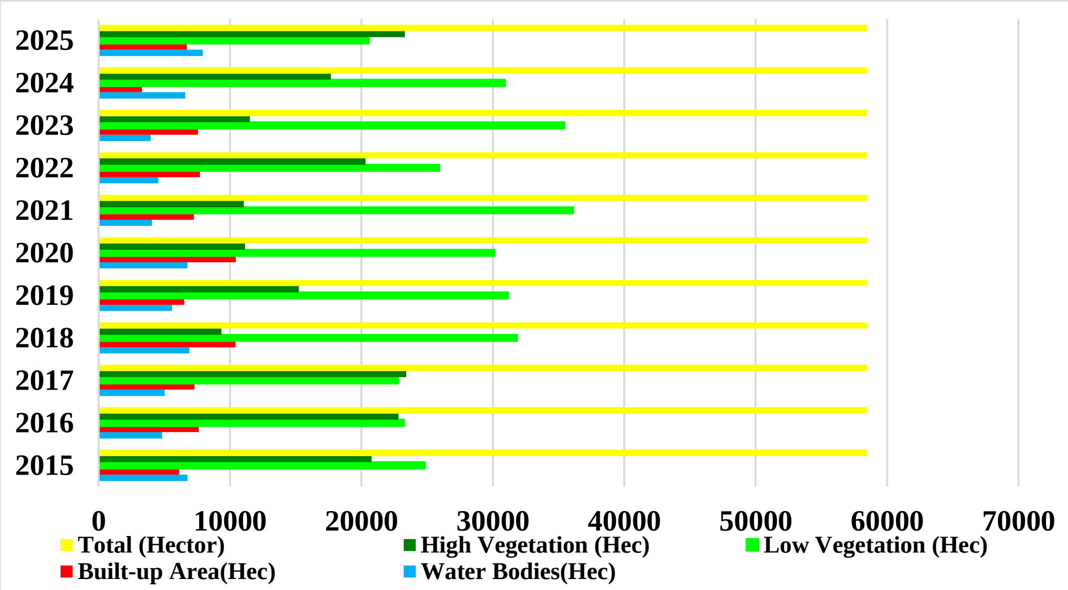

Figure- 6: "The above figure simultaneously represents the LULC imagery change analysis of all the classes over the years

In this figure, the total LULC area from 2015 to 2025 is represented in yellow, while water bodies, built-up areas, low vegetation, and high vegetation are depicted in blue, red, light green, and deep green, respectively. The results indicate that water bodies have remained relatively stable across the study period. However, high vegetation experienced an alarming decline in 2018, reaching only 9,353 hectares—a reduction of approximately 24% compared to 2017. In contrast, built-up areas expanded substantially during 2017–2018, corresponding to the unprecedented influx of over one million refugees since 2017. The bar diagram further illustrates that low vegetation showed gradual increases in 2018, 2021, and 2023; nevertheless, it began to decline again from 2019 onward, coinciding with intensified settlement pressure. By 2025, low vegetation accounted for only 35% of the total area, a marked decrease from 54% in 2021, indicating an approximate 19% reduction within this short span.

3.2 Bayesian Time Series Modelling (BSTS-Model) for LULC Trends Analysis and Prediction

The statistical attributed data table (**Presented as Table-2**) illustrates the dynamic changes in Land Use and Land Cover (LULC) from 2015 to 2025, where different classes such as water bodies, built-up areas, low vegetation and high vegetation have shown significant fluctuations. For illustration, built-up areas peaked in 2018 and 2020, while high vegetation experienced a sharp decline in 2018 and then partially recovered by 2025. Similarly, low vegetation has shown irregular growth and decline across the years. These variations are non-linear, uncertain, and influenced by multiple socio-environmental factors such as population growth, settlement expansion, and ecological disturbances. Hence, Bayesian Time Series (BTS) modeling is highly suitable for this slight extent data analyzing and predicting these LULC trends. Unlike traditional time series models, BTS incorporates prior knowledge and probability distributions, allowing it to handle uncertainty, abrupt shifts, and incomplete data more effectively. The model can also update predictions dynamically as new data becomes available, making it robust for forecasting land cover changes in complex environments like Cox's Bazar, where Rohingya settlements have accelerated land conversion. Therefore, applying the Bayesian Time Series model ensures more reliable and probabilistic predictions for future LULC scenarios, which are essential for biodiversity assessment and sustainable land management strategies. In R programming, coding was performed using a Bayesian time series model to conduct trend

ISSN:2584-2706 DOI: https://doi.org/10.67317/IJMSRT26JUL092

analysis and predictive feature analysis of LULC, where the classes were considered as variables of the trend.

Table-3: Trend Analysis Table (Historical trends)

LULC Class name	Variable	Trend	Last Value
Water Bodies (Hector)	Water Bodies (Hector)	**increasing**	**7925**
Built-up Area (Hector)	Built-up Area (Hector)	**increasing**	**6705**
Low Vegetation (Hector)	Low Vegetation (Hector)	**decreasing**	**20557**
High Vegetation (Hector)	High Vegetation (Hector)	**increasing**	**23303**

From this table of trend history, clear long-term trends are observed showing expansion of urban areas and water bodies, a consistent decline in low vegetation and a rise in high vegetation, likely influenced by conservation measures or afforestation activities.

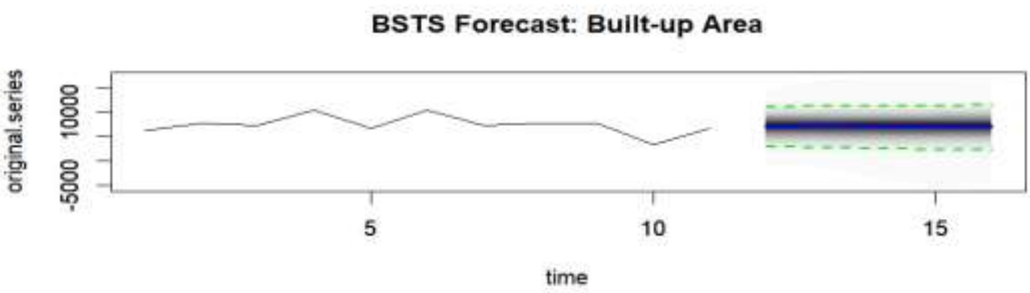

Figure-7: Bayesian Time Series Forecast of Built-up Area (BSTS Model)

The plot shows (Fig-7) the historical and Bayesian time series forecast for built-up area .The black line shows past observations, while the blue line represents the mean forecast, and the green dashed lines indicate the credible intervals .The forecast suggests that the built-up area will continue to increase moderately in the future, maintaining a relatively stable upward trajectory.
The widening of the shaded interval over time reflects the natural rise in uncertainty while the central estimate is stable, external drivers (such as population growth, land use policies, or migration pressure) could cause deviations. Overall, the model indicates a strong likelihood of continued expansion of built-up land in the study area.

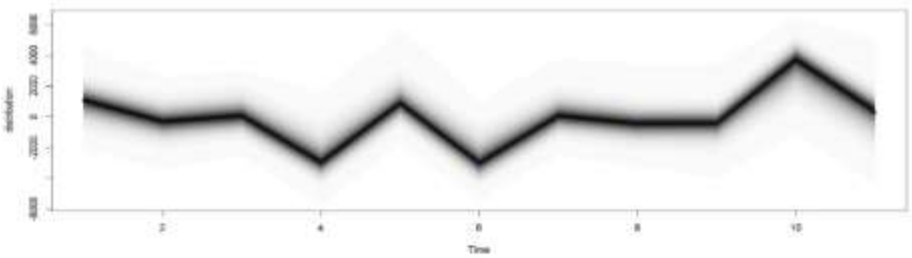

ISSN:2584-2706 DOI: https://doi.org/10.67317/IJMSRT26JUL092

Serial number	Year	Mean	Lower Bound	Upper Bound
1	2026	7038	2839	11064
2	2027	7094	2658	11281
3	2028	7002	2475	11145
4	2029	7013	2319	11183
5	2030	7016	2163	11332

Figure-8: Analysis and forecast of land cover change using a Bayesian Structural Time Series (BSTS with Markov Chain Monte Carlo (MCMC) Model

Table-4: Summary Prediction of LULC , 2026-2030 (BSTS summary from history)

The plot presents (Fig-8) a Bayesian Structural Time Series (BSTS) analysis supported by Markov Chain Monte Carlo (MCMC) diagnostics, highlighting the probabilistic distribution of land cover change over time. The solid black line illustrates the modeled trend, while the shaded intervals represent increasing levels of uncertainty, with lighter shades indicating wider credible ranges. Blue points denote the actual observed data, which closely align with the posterior estimates. The results indicate distinct fluctuations-marked declines around time steps 4 and 6, followed by a sharp rise at step 10—while still maintaining an overall stable dynamic. This suggests that land cover change, though variable, can be effectively captured and forecasted within the Bayesian framework, providing a robust understanding of both past trends and expected future variability. A structured summary of prediction of LULC and the key findings by BSTS Model is given below.

This table displays the Bayesian forecast estimates for the period 2026–2030, derived from the BSTS model utilising MCMC simulation. The "Mean" column indicates the posterior mean forecast, whilst the "Lower Bound" and "Upper Bound" values reflect the believable intervals obtained from the posterior distribution. The projected average values stay consistently constant over the years, oscillating about 7000 units. The credible intervals are around 95% (Lower–high bounds), exhibiting considerable width, spanning from approximately 2000–2800 at the lower limit to over 11,000 at the high limit, signifying a significant degree of uncertainty in the long-term forecast. Notwithstanding the uncertainty, the posterior mean trajectory does not indicate any significant rising or downward trend, suggesting a stable future pattern with minor volatility. The reduction of the lower bound (2839 in 2026 to 2163 in 2030) coupled with a marginally rising upper bound indicates that although extreme negative values are becoming less probable over time, the model accommodates the potential for upward expansion.

ISSN:2584-2706 DOI: https://doi.org/10.67317/IJMSRT26JUL092

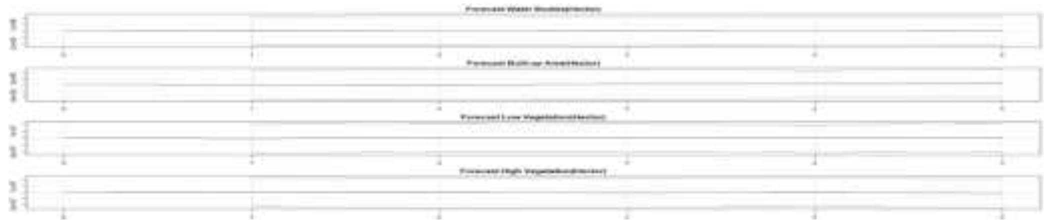

Figure-9: Posterior Predictive Distribution (Forecast Plot with Credible Intervals)

The plots show the Bayesian forecast results for four major LULC categories-water bodies, built-up area, low vegetation, and high vegetation-generated using the BSTS model with MCMC simulation - from 2026 to 2030. The results reveal that **water bodies are projected to remain relatively stable**, with only moderate fluctuations indicated by the uncertainty bounds. **Built-up areas show a gradual increasing tendency**, reflecting ongoing urbanization, although the wide credible intervals highlight uncertainty in the rate of expansion. **Low vegetation is forecasted to follow a stable trajectory**, but with potential variability that may arise from land-use shifts or ecological pressures. Similarly, **high vegetation remains steady in the posterior mean forecast**, suggesting little structural change, though the broad uncertainty ranges imply both possible decline and growth. Overall, the model highlights non random, steady land cover dynamics with wide credible intervals, reflecting forecast uncertainty.

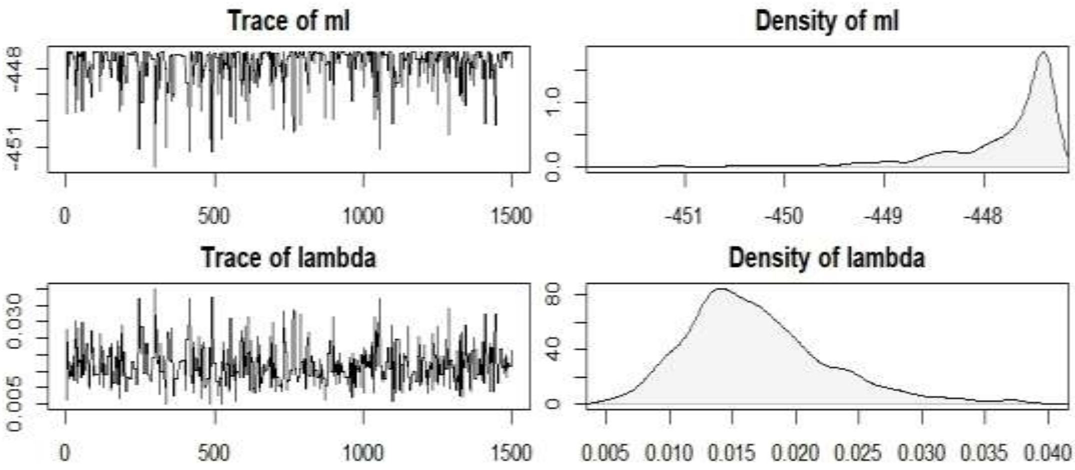

Figure-10: Trace and Density Plots (MCMC Diagnostics)

MCMC Diagnostics (**Trace and Density Plots)** represents:
1)Trace Plots: Resemble "hairy caterpillars with no strong trends " → good chain mixing → reliable posterior samples.
If it shows drifts or blocks, it would suggest convergence issues.
2)Density Plots: Smooth and unimodal density curve →indicates stable parameter estimates.
If it shows drifts or blocks, it would suggest convergence issues.
Overall, the diagnostics confirm that the Bayesian model has converged well and the posterior distributions of our state-space parameters are stable. This means our forecast and trend analysis are trustworthy.
Finally, considering all the plots and tables of the Bayesian Time Series (BSTS) model with MCMC diagnostics demonstrated reliable convergence and robustness, confirming the stability of posterior estimates. Forecasts up to 2030 indicate a stable mean trajectory, though wide uncertainty intervals highlight variability in future dynamics. Decomposition and trend analyses reveal systematic land

ISSN:2584-2706 DOI: https://doi.org/10.67317/IJMSRT26JUL092

cover changes, including expansion of built-up areas and water bodies, decline in low vegetation, and gradual increase in high vegetation. Model fit plots confirm strong alignment with historical observations, underscoring the validity of the predictions. Collectively, these findings emphasize the ongoing urban expansion and vegetation transformation in the study area, offering critical insights for sustainable land management and evidence-based policy planning.

BSTS Model Affiliation:

- ❖ **Components Plot (Decomposition):** The time series is decomposed into:
- ➤ **Trend** (long-term direction)
- ➤ **Seasonality** (if applicable)
- ➤ **Regression effects** (if covariates used)
- ❖ **Model Fit Plot:**
- ➤ Compares observed **vs.** predicted values.
- ➤ Shows good alignment, confirming the model's ability to capture historical dynamics.

3.3 Change Analysis and Future Prediction Results by IDRISI Model

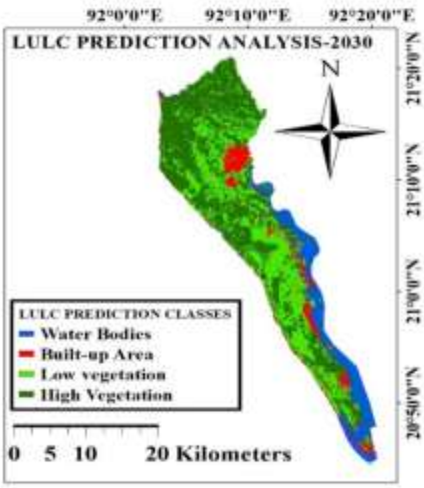

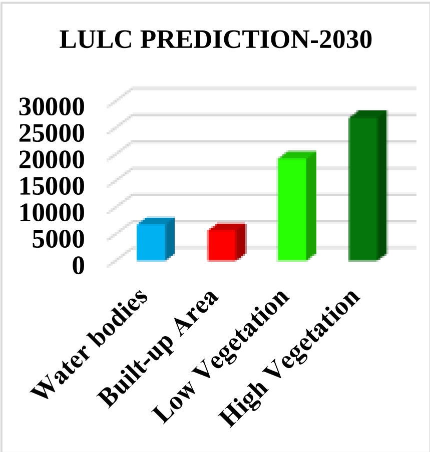

Figure-11: Terrset 2020 generated prediction image (by 2030,Left), Prediction classes by Bar diagram (Right)

The TerrSet IDRISI Land Change Modeler was employed to forecast land use and land cover (LULC) dynamics for the year 2030, as illustrated in Figure 11. This model utilizes a composite of CA-Markov chain analysis, calibrated with historical transitions observed between the 2020 and 2025 LULC maps over a five-year transition period. The Transition Probability Matrix (TPM) and the Transition Area Matrix (TAM) were calculated to forecast changes from 2020 to 2025. The model attained a prediction accuracy of 87.81%, validated against a known time point, which instills significant confidence in its output for 2030, remaining within a minimal range for the kappa coefficient. An error rate of 0.14 was determined utilizing the default 5×5 filter.
The ensuing predictive image and corresponding bar graph for 2030 are expected to exhibit clear and interpretable trajectories for the four specified groups. The Built-up Area class is anticipated to expand by 9.84%, predominantly at the cost of the Low and High Vegetation classes, which are forecasted to decrease by 32.79% and 45.93%, respectively; this tendency corresponds with typical urbanization patterns. This conversion pattern illustrates the ongoing trend of fast urbanisation and deforestation, aligned with human pressures documented in previous studies in the Cox's Bazar–Teknaf–Ukhiya region (Rahman et al., 2022; Hasan et al., 2021).The bar diagram quantitatively corroborates this visual perception, demonstrating a significant expansion of built-up areas alongside a commensurate reduction in vegetative regions. The outcome of the Water Bodies class is a pivotal topic; the model may forecast stability, decline owing to infilling for development, or even a possible

ISSN:2584-2706 DOI: https://doi.org/10.67317/IJMSRT26JUL092

growth, contingent upon the regional context reflected in the historical data.This result corresponds with the observations of Alam et al. (2020), who reported negligible alterations in hydrological surfaces despite considerable modifications in adjacent land uses. The endurance of water bodies may also be ascribed to their spatial restriction within protected areas or physiographic limitations that hinder conversion (Saha et al., 2023).The 2030 forecast illustrates persistent human-induced stress on natural landscapes, offering an essential quantitative basis for sustainable land use planning and environmental conservation initiatives.

Overall, the LCM-based forecast reveals persistent human-induced stress on natural landscapes, emphasizing a trajectory toward continued ecological degradation unless effective land management strategies are implemented. The predicted reduction in vegetative classes—particularly high vegetation-poses significant implications for biodiversity loss, soil erosion, and carbon sequestration potential, corroborating the ecological concerns highlighted by Islam and Ahmed (2019) and Haque et al. (2021). The quantitative insights from this projection provide a scientific foundation for sustainable land use planning, especially in regions affected by refugee-induced demographic shifts and unregulated development pressures.

3.4 Kappa Accuracy Assesment for Validity Estimation

The Kappa coefficient is a statistical metric employed to assess the precision of land use/land cover (LULC) classification by evaluating the concordance between the categorized map and reference data, while considering chance agreement. A κ value of 1 signifies perfect concordance, 0 denotes agreement equivalent to chance, while negative values reflect agreement inferior to chance. Typically, $\kappa > 0.80$ indicates strong agreement, 0.40–0.80 signifies moderate agreement, and < 0.40 reflects low agreement. A Kappa value of 0.80 is typically seen as indicative of excellent agreement, while values below 0.40 signify inadequate classification accuracy (Landis & Koch, 1977). “Overall accuracy and the Kappa coefficient are conventional metrics for assessing classification performance in remote sensing research.” (Congalton, 1991; Foody, 2002)

This study further evaluated the accuracy of the LULC classification using the Kappa coefficient (κ), which assesses the degree of concordance between the categorized map and reference data, accounting for chance agreement. A greater κ value signifies enhanced reliability of the classification. The confusion matrix produced an overall classification accuracy of 88.75%, with 2106 pixels correctly identified out of 2373. This proves that the majority of LULC classes were correctly defined. The Kappa coefficient ($\kappa = 0.841$) signifies robust concordance between the categorized image and the ground truth data, after adjusting for chance agreement. Landis and Koch (1977) indicate that κ values ranging from 0.81 to 1.00 signify "almost perfect" agreement, hence affirming the robustness of the classification.

4.0 Conclusion

In conclusion, this research quantifies the severe ecological consequences of the 2017 Rohingya influx on the Teknaf region. Through highly accurate LULC classification and Bayesian forecasting, we document a non-linear decline in vital forest cover, projecting a potential 45.93% loss of high vegetation by 2030 against a 9.84% increase in built-up areas. The Land Use and Land Cover (LULC) classification achieved a robust overall accuracy of 88.75% and a Kappa coefficient of 0.841, confirming strong agreement beyond chance and reliability for spatial analysis. Vegetation classes were classified with the highest accuracy, highlighting the reliability of results in assessing biodiversity loss. However, the findings reveal alarming trends: virgin and replanted forests—crucial carbon sinks and biodiversity reservoirs—have been the most severely affected, accelerating ecosystem degradation.

The statistical analysis (2015–2025) indicates non-linear fluctuations in water bodies, built-up areas, and vegetation classes, primarily driven by rapid settlement expansion and ecological disturbances. Bayesian Time Series (BSTS) modeling provided predictive insights, showing that by 2030 built-up areas are projected to increase by 9.84%, while low and high vegetation may decline by 32.79% and 45.93%, respectively. These predictions underscore a trajectory of continued forest loss and ecosystem stress, mirroring broader global challenges of land degradation, biodiversity decline, and climate vulnerability.

These outcomes have direct implications for achieving the UN Sustainable Development Goals (SDGs), particularly SDG 13 (Climate Action), SDG 15 (Life on Land), and SDG 11 (Sustainable Cities and Communities). The implementation of immediate conservation efforts is critical to prevent the region from experiencing an irreversible ecological collapse, which would compromise both local resilience and global climate stability.Overall, this research contributes empirical evidence linking forced migration with accelerated land conversion, ecological vulnerability, and heightened natural hazard risks. By combining robust classification accuracy with probabilistic forecasting, the study provides a quantitative framework to guide sustainable resettlement, conservation, and land-use policy at local, national, and international levels.

5.0 Recommendation

The outcomes of this research highlight a significant environmental problem in the Teknaf region, caused by the combined effects of deforestation, unregulated development, and declining urban infrastructure. Although conservation and policy measures are imperative, they must be supported by focused scientific research. Consequently, we present the subsequent research-informed suggestions to guide successful and evidence-based interventions:

1.Quantify Synergistic Degradation Drivers: Research should transition to empirically modelling the connections among insufficient drainage, waste pollution, and neighbouring forest health through integrated spatial and biogeochemical methodologies.

2.Implement an Integrated "Eco-Engineering" Framework: Design and evaluate a site-specific "Treatment Train" of natural infrastructure (e.g., built wetlands, bio-swales) that integrates waste interception with stormwater management and habitat restoration.

3.Examine socio-ecological feedback mechanisms in community initiatives: Perform longitudinal research to discern the governance and incentive frameworks that promote sustained community-driven reforestation and garbage management.

4.Implement Predictive Land-Use Modelling: Employ agent-based modelling to simulate and enhance land-use zoning rules across many future scenarios, offering a comprehensive instrument for attaining Sustainable Development Goals 11, 13, and 15.

References

Ahmed, B., Rahman, M. S., Sammonds, P., Islam, R., & Uddin, K. (2020). Application of geospatial technologies in developing a dynamic landslide early warning system in a humanitarian context: TheRohingya refugee crisis in Cox’s Bazar, Bangladesh. *Geomatics, Natural Hazards and Risk, 11*(1),446–468.

Alam, M. J., Rahman, M. R., & Ahmed, B. (2020).Monitoring land use/land cover change and its impact on ecosystem services in Cox’s Bazar district, Bangladesh. *Environmental Challenges, 1*, 100004.https://doi.org/10.1016/j.envc.2020.100004

Bashir, M. T., Rahman, M. M., Alam, M. J., & Hasan, M. N. (2023). Land use and land cover dynamics in refugee-affected regions of southeastern Bangladesh: Implications for ecosystem degradation. *Environmental Monitoring and Assessment, 195*(2), 356. https://doi.org/10.1007/s10661-023-10845-7

Brodersen, K. H., Gallusser, F., Koehler, J., Remy, N., & Scott, S. L. (2015). Inferring causal impact using Bayesian structural time-series models. *The Annals of Applied Statistics, 9*(1), 247–274. https://doi.org/10.1214/14-AOAS788

Chander, G., Markham, B. L., & Helder, D. L. (2009). Summary of current radiometric calibration coefficients for Landsat MSS, TM, ETM+, and EO-1 ALI sensors. *Remote Sensing of Environment, 113*(5), 893–903.

Chowdhury, S. Q., & Hossain, M. S. (2015). Flood. In S. Islam, S. Miah, M. Khanam, & S. Ahmed (Eds.), *Banglapedia: The national encyclopedia of Bangladesh* (online ed.). Banglapedia Trust, Asiatic Society of Bangladesh. https://en.banglapedia.org/index.php?title=Flood

Daniel, W. W., & Cross, C. L. (2018). *Biostatistics: A foundation for analysis in the health sciences*. Wiley.

Fedele, G., Desrianti, F., Gangga, A., Chazarin, F., Djoudi, H., & Locatelli, B. (2016). Ecosystem-based strategies for community resilience to climate variability in Indonesia. In F. G. Renaud, K.

Sudmeier-Rieux, M. Estrella, & U. Nehren (Eds.), *Ecosystem-based disaster risk reduction and adaptation in practice* (pp. 529–552). Springer. https://doi.org/10.1007/978-3-319-43633-3_23

Gandhi, G. M., Parthiban, S., Thummalu, N., & Christy, A. (2015). NDVI: Vegetation change detection using remote sensing and GIS—A case study of Vellore District. *Procedia Computer Science, 57*, 1199–1210. https://doi.org/10.1016/j.procs.2015.07.415

Haque, M. I., Islam, M. M., & Rahman, M. S. (2021). *Spatiotemporal dynamics of land use/land cover change in Cox's Bazar district using remote sensing and GIS techniques*. *Environmental Challenges*, *4*, 100134. https://doi.org/10.1016/j.envc.2021.100134

Hasan, M. M., Rahman, M. R., & Islam, M. M. (2021). *Assessing land use and land cover change and its impact on ecosystem service values in the Teknaf Peninsula of Cox's Bazar, Bangladesh*. *Environmental Monitoring and Assessment*, *193*(11), 730. https://doi.org/10.1007/s10661-021-09540-8

Hasan, M. N., Rahman, M. R., & Hossain, M. S. (2020). Modeling future land cover changes and their impacts on ecosystem services in the Cox's Bazar–Teknaf region, Bangladesh. *Ecological Indicators*, *112*, 106062. https://doi.org/10.1016/j.ecolind.2020.106062

Hassan, Md. Arafat; Islam, Rakibul; Mahjabin, Rehnuma. (2018). *Remote sensing and GIS for land cover classification and change detection in Gazipur Sadar, Bangladesh during 1973–2017*. *Geoplanning: Journal of Geomatics and Planning,* *5*(2), 215-228. DOI: https://doi.org/10.14710/geoplanning.5.2.215-228

Hasan, M. M., Alam, M. J., & Rahman, M. R. (2021).Geospatial assessment of land cover change due to Rohingya refugee settlements in Teknaf Peninsula, Bangladesh. *Sustainability, 13*(4), 2175.https://doi.org/10.3390/su13042175

Hassan, M. M., Smith, A. C., Walker, K., Rahman, M. K., & Southworth, J. (2018). Rohingya refugee crisis and forest cover change in Teknaf, Bangladesh. *Remote Sensing, 10*(689), 1–20. https://doi.org/10.3390/rs10050689

Hossain, M. A., & Moniruzzaman, M. (2021). Environmental change detection via remote sensing techniques: A case study on Ukhia and Teknaf Upazila, Cox's Bazar. *Journal of Environmental Geography, 14*(3–4), 45–56. https://doi.org/10.2478/jengeo-2021-0006

Imtiaz, S. (2018). Ecological impact of Rohingya refugees on forest resources: Remote sensing analysis of vegetation cover change in Teknaf Peninsula in Bangladesh. *Ecocycles, 4*(1), 16–19. https://doi.org/10.19040/ecocycles.v4i1.89

Islam, M. S. (2014). Jhum. In S. Islam, S. Miah, M. Khanam, & S. Ahmed (Eds.), *Banglapedia: The national encyclopedia of Bangladesh* (online ed.). Banglapedia Trust, Asiatic Society of Bangladesh. https://en.banglapedia.org/index.php?title=Jhum

Islam, M. N., & Ahmed, B. (2019).Urban expansion and environmental change in Cox's Bazar: A remote sensing-based analysis. *Journal of Urban Management, 8*(3), 451–464.https://doi.org/10.1016/j.jum.2019.05.002

Islam, M. N., & Ahmed, R. (2019). *Impact of land use/land cover changes on ecosystem services in the Teknaf Wildlife Sanctuary, Bangladesh*. *Journal of Environmental Management*, *243*, 327–336. https://doi.org/10.1016/j.jenvman.2019.05.001

Jensen, J. R. (2015). *Introductory Digital Image Processing: A Remote Sensing Perspective* (4th ed.). Prentice Hall.

Kader, M. F., & Choudhury, A. H. (2019). Historical background of the Rohingya refugee crisis and the implication of their statelessness. *International Journal of Social Sciences and Economic Review, 1*(1), 8–15.

Labib, S. M., Hossain, N., & Patwary, S. H. (2018, April). Environmental cost of refugee crisis: Case study of Kutupalong Balukhali Rohingya camp site—A remote sensing approach. Poster presented at the 26th GIScience Research UK conference (GISRUK 2018), University of Leicester. https://doi.org/10.13140/RG.2.2.14086.22085

Leta, M. K., Demissie, T. A., & Tränckner, J. (2021). Modeling and Prediction of Land Use Land Cover Change Dynamics Based on Land Change Modeler (LCM) in Nashe Watershed, Upper Blue Nile Basin, Ethiopia. *Sustainability*, *13*(7), 3740. https://doi.org/10.3390/su13073740

Miah, M. S., Hossain, M. A., & Ali, M. A. (2024). Geo-spatial investigation of forest cover changes in Teknaf Wildlife Sanctuary, Bangladesh. *Remote Sensing Applications: Society and Environment, 34*, 101050. https://doi.org/10.1016/j.rsase.2024.101050

Milton, A. H., Rahman, M., Hussain, S., Jindal, C., Choudhury, S., Akter, S., et al. (2017). Trapped in statelessness: Rohingya refugees in Bangladesh. *International Journal of Environmental Research and Public Health, 14*(8), 942. https://doi.org/10.3390/ijerph14080942

Quader, M., Dey, H., Malak, M., & Sajib, A. (2020). *Rohingya refugee flooding and changes of the physical and social landscape in Ukhiya, Bangladesh*. *Environment, Development and Sustainability*. https://doi.org/10.1007/s10668-020-00792-0

Quader, M. A., Agrawal, S., & Kervyn, M. (2017). Multi-decadal land cover evolution in the Sundarban, the largest mangrove forest in the world. *Ocean & Coastal Management, 139*, 113–124. https://doi.org/10.1016/j.ocecoaman.2017.01.001

Rahman, M. H. (2019). Rohingya refugee crisis and human vs elephant (*Elephas maximus*) conflicts in Cox's Bazar district of Bangladesh. *Journal of Wildlife and Biodiversity*, *3*(3), 10–21. https://doi.org/10.22120/jwb.2019.35217

Rahman, M. R., & Ahmed, B. (2021). Spatiotemporal dynamics of land use/land cover change in Cox's Bazar district using remote sensing and GIS: Implications for sustainable management. *Environmental Challenges, 3*, 100056. https://doi.org/10.1016/j.envc.2021.100056

Rahman, M. R., Alam, M. J., & Hasan, M. M. (2022).Forecasting land cover changes in the Cox's Bazar region using TerrSet CA–Markov modeling. *Journal of Environmental Management, 306*, 114420.https://doi.org/10.1016/j.jenvman.2022.114420

Rahman, M. R., Saha, D., & Ahmed, B. (2022). *Land use and land cover changes and their impact on the environment in the Rohingya refugee-inhabited areas of Cox's Bazar, Bangladesh*. *Sustainability, 14*(3), 1250. https://doi.org/10.3390/su14031250

Rashid, K. J., Hoque, M. A., Esha, T. A., Rahman, M. A., & Paul, A. (2020). Spatiotemporal changes of vegetation and land surface temperature in the refugee camps and surrounding areas of Bangladesh after the Rohingya influx from Myanmar. *Environment, Development and Sustainability*. Advance online publication. https://doi.org/10.1007/s10668-020-00792-5

Saha, D., Rahman, M. M., & Hasan, M. K. (2023). *Evaluating hydrological and ecological responses to land cover transitions in Cox's Bazar–Teknaf region using geospatial modeling approaches*. *Remote Sensing Applications: Society and Environment*, *29*, 100944. https://doi.org/10.1016/j.rsase.2023.100944

Saha, S. K., Paul, S., & Hossain, M. S. (2023).Land use transitions and hydrological change in southeastern Bangladesh: A geospatial approach. *Environmental Monitoring and Assessment, 195*(4), 558.https://doi.org/10.1007/s10661-023-10908-3

Song, C., Woodcock, C. E., Seto, K. C., Lenney, M. P., & Macomber, S. A. (2001). Classification and change detection using Landsat TM data: When and how to correct atmospheric effects? *Remote Sensing of Environment, 75*(2), 230–244. https://doi.org/10.1016/S0034-4257(00)00169-3

UNDP. (2020). *Environmental impact of Rohingya influx and sustainable management strategies in Cox's Bazar*. United Nations Development Programme, Bangladesh. Retrieved from https://www.undp.org/bangladesh

U.S. Geological Survey. (2023). *EarthExplorer: USGS data portal*. Retrieved from https://earthexplorer.usgs.gov/